

# Quantitative Ultrasound Assessment of Hepatic Steatosis



Artem Kaliaev\*, Wilson Chavez\*, Jorge Soto\*, Fahimul Huda\*, Hua Xie†, Man Nguyen†, Vijay Shamdasani‡, Stephan Anderson\*

\*Boston University Medical Center, Department of Radiology, Boston, MA, USA, †Ultrasound Imaging and Interventions, Philips Research North America, Cambridge, MA, USA and ‡Philips Healthcare, Bothell, WA, USA

**Background/Aims:** Non-alcoholic fatty liver disease (NAFLD) is widespread chronic disease of the live in humans with the prevalence of 30% of the United States population.<sup>1,2</sup> The goal of the study is to validate the performance of quantitative ultrasound algorithms in the assessment of hepatic steatosis in patients with suspected NAFLD.

**Methods:** This prospective study enrolled a total of 31 patients with clinical suspicion of NAFLD to receive liver fat measurements by quantitative ultrasound and reference MRI measurements (proton density fat-fraction, PDFF). The following ultrasound (US) parameters based on both raw ultrasound RF (Radio Frequency) data and 2D B-mode images of the liver were analyzed with subsequent correlation with MRI-PDFF: hepatorenal index, acoustic attenuation coefficient, Nakagami coefficient parameter, shear wave viscosity, shear wave dispersion and shear wave elasticity. Ultrasound parameters were also correlated with the presence of hypertension and diabetes. **Results:** The mean ( $\pm$  SD) age and body mass index of the patients were 49.03 ( $\pm$  12.49) and 30.12 ( $\pm$  6.15), respectively.

Of the aforementioned ultrasound parameters, the hepatorenal index and acoustic attenuation coefficient showed a strong correlation with MRI-PDFF derivations of hepatic steatosis, with *r*-values of 0.829 and 0.765, respectively. None of the remaining US parameters showed strong correlations with PDFF. Significant differences in Nakagami parameters and acoustic attenuation coefficients were found in those patients with and without hypertension. **Conclusions:** Hepatorenal index and acoustic attenuation coefficient correlate well with MRI-PDFF-derived measurements of hepatic steatosis. Quantitative ultrasound is a promising tool for the diagnosis and assessment of patients with NAFLD. (J CLIN EXP HEPATOL 2022;12:1091-1101)

Non-alcoholic fatty liver disease (NAFLD) is widespread chronic disease of the live in humans, and its prevalence continues to rise.<sup>1</sup> The prevalence of NAFLD approaches 30% of the United States population and is closely linked to metabolic disorders, such as metabolic syndrome, insulin resistance (IR), type 2 diabetes mellitus (T2DM), obesity, hyperinsulinemia, and cardiovascular disease.<sup>2</sup> While it has long been known that NAFLD may progress to end-stage liver disease, more recently, the degree of risk has been more clearly defined.<sup>3</sup> Furthermore, NAFLD complications represent a tremendous economic burden with an estimated annual cost of \$103 billion in

the United States, resulting in an average cost of \$1613 per patient, with over 64 million people affected.<sup>4</sup>

Liver biopsy has traditionally represented the gold standard in NAFLD detection, quantification, and characterization. However, the inherent limitations of liver biopsy include its invasive nature and sampling bias since percutaneous biopsies sample as little as 1/50,000 of the total mass of the liver, resulting in undersampling and potentially inaccurate diagnosis.<sup>5</sup> Furthermore, the evaluation of liver biopsy is subjective, and therefore, dependent on the experience of the interpreting pathologist, with well-known rates of intra- and inter-observer variability.<sup>6</sup>

Given the limitations of liver biopsy, non-invasive imaging techniques have been developed to assess diffuse liver diseases. Among these, magnetic resonance imaging (MRI) with proton density fat fraction (PDFF) has been reported to have a high degree of accuracy in quantifying liver steatosis.<sup>7</sup> However, MRI is fundamentally expensive and not universally accessible. Another reported US-based method to detect liver steatosis is the Fibroscan-derived controlled attenuation parameter (CAP), which has demonstrated diagnostic utility in fibrosis and may be used for the diagnosis of hepatic steatosis.<sup>8</sup>

Finally, ultrasound (US) imaging is also readily available and relatively inexpensive, when compared to MRI. Recent

**Keywords:** non-alcoholic fatty liver disease, ultrasound, liver fat quantification

Received: 4.12.2020; Accepted: 17.1.2022; Available online 31 January 2022

Address for correspondence: Artem Kaliaev, Department of Radiology, Boston University Medical Center, 820 Harrison Ave, Boston, MA 02118, USA.

E-mail: akaliaev@bu.edu

**Abbreviations:** ALT: alanine aminotransferase; AST: aspartate aminotransferase; BMI: body mass index; DICOM: digital imaging and communications in medicine; Hgb A1C: hemoglobin A1C (glycated hemoglobin); HIPAA: health insurance portability and accountability act; HRI: hepatorenal index; IQ: in-phase quadrature; IR: insulin resistance; LDL: low-density lipoprotein; MRI-PDFF: magnetic resonance imaging - proton density fat-fraction; NAFLD: non-alcoholic fatty liver disease; NASH: non-alcoholic steatohepatitis; RF: raw radio frequency; ROI: regions of interest; SD: standard deviation; T2DM: type 2 diabetes mellitus; US: ultrasound

<https://doi.org/10.1016/j.jceh.2022.01.007>

reports support the potential for US in quantifying hepatic steatosis.<sup>9,10</sup>

The purpose of this study is to explore further the clinical performance of ultrasound in quantifying hepatic steatosis in comparison to the reference standard of MRI-PDFF in patients with suspected NAFLD.

## MATERIAL AND METHODS

### Study Design

This is a prospective, single-site study of liver fat quantification using quantitative 2D ultrasound. Between September 2018 and May 2019, 31 adult patients undergoing clinically-indicated pelvic or abdominal ultrasounds were consecutively enrolled. The Institutional Review Board approved this HIPAA compliant study. All participants gave written informed consent for their participation in accordance with the Declaration of Helsinki.

### Inclusion/Exclusion Criteria

We included adult patients  $\geq$  18-years-old with clinically-suspected NAFLD who were willing and able to provide informed consent to participate in all parts of the study. NAFLD suspicion was based on a subjective assessment of an abnormally echogenic liver at the time of the patient's clinically-indicated ultrasound, laboratory abnormalities such as levels of aspartate aminotransferase, alanine aminotransferase, high- and low-density lipoproteins, or hemoglobin A1C (glycated hemoglobin) suggesting hepatic steatosis, or correlated risk factors including obesity, diabetes mellitus type 2, and hypertension. Exclusion criteria included the following: a history of moderate or heavy alcohol consumption (i.e.,  $> 20$  g or  $> 2$  glasses of alcohol per day for women, and  $> 30$  g or  $> 3$  glasses of alcohol per day for men); any ultrasound or prior imaging evidence of advanced liver fibrosis or cirrhosis and solid liver lesions or liver cancer; known chronic liver diseases such as viral/cholestatic or autoimmune; diseases requiring the use of drugs associated with steatosis, such as amiodarone or methotrexate; exposure to known hepatotoxins such as  $\alpha$ -amanitin, aflatoxins, carbon tetrachloride, etc.; contraindication(s) to MRI; pregnant or attempting to become pregnant. Also, notably, none of the patients in this cohort had any evidence of renal disease, hemochromatosis, or ascites.

### Ultrasound Imaging and Data Processing

Ultrasound data collection was performed using a Philips EPIQ 7G ultrasound system equipped with shear wave elastography and a C5-1 curvilinear transducer (Philips Healthcare, Andover, MA). Besides Digital Imaging and

Communications in Medicine (DICOM) images, raw radio frequency (RF) or in-phase quadrature (IQ) data were also captured for offline calculation of five ultrasound-derived parameters: hepatorenal index (HRI), acoustic attenuation coefficient, Nakagami coefficient, shear wave viscosity, and shear wave dispersion, detailed further below.

Hepatorenal index (HRI) is a metric that calculates the ultrasound intensity contrast between the liver and the right kidney. During this analysis, a pair of regions of interest (ROIs) were placed at the same image depth, one within the liver parenchyma and the other in the right kidney cortex. HRI is the ratio between the averaged echo-intensity in liver ROI and kidney ROI. Excessive fat infiltration in the liver increases the acoustic backscattering coefficient leading to higher greyscale values in the near field and mid-field in ultrasound B-mode imaging. In this study, HRI was calculated using two types of co-registered data: DICOM and RF.<sup>11-13</sup>

Acoustic attenuation coefficient is a measure of the ultrasound signal intensity decrease-rate as a function of propagation distance and frequency. As fat is more attenuating than healthy liver tissue, the acoustic attenuation coefficient is expected to increase with an increase in liver fat.<sup>14,15</sup>

The Nakagami coefficient parameter describes speckle statistics governed by backscattered distribution characteristics. Liver parenchyma may be modeled as a collection of scatterers with microstructures in dimensions smaller than the acoustic wavelength. The ultrasound envelope signal for healthy liver tissues typically follows a pre-Rayleigh or Rayleigh distribution. With increasing hepatic fat, variations in backscatter concentrations and arrangements are expected to lead to Rayleigh or post-Rayleigh probability density functions (PDF). The Nakagami coefficient parameter is employed as a metric to differentiate pre-Rayleigh, Rayleigh, and post-Rayleigh distributions. As the liver progresses from healthy to steatotic, a higher Nakagami coefficient is expected, indicating backscattered statistics transitioning from pre-Rayleigh to Rayleigh and post-Rayleigh distributions. Nakagami coefficients were calculated to investigate frequency dependence of the backscattered statistics in livers with different stages of steatosis, by using both Nakagami fundamental and harmonic signals. In the case of Nakagami harmonic images, the area of the sliding windows is reduced by a factor of 4, while the sliding step is reduced by a factor of 2 compared to the Nakagami fundamental images.<sup>16-19</sup>

As soft tissue is a mixture of solid and liquid components, and elasticity may be employed to characterize the resistance to deformation due to an external force applied to the solid portion of tissue, viscosity characterizes the resistance to deformation due to an external force applied to the liquid portion of biological tissue. Some early

preclinical studies supported the hypothesis that increased liver fat content will lead to higher viscosity and stronger degrees of dispersion.<sup>20,21</sup> In this study, the commercial shear wave elastography feature (ElastQ, Philips Healthcare, Andover, MA) was employed to generate broadband shear waves in the liver, allowing for shear wave phase velocity at different frequencies to be estimated, which subsequently leads to shear viscosity reconstruction by Voigt model fitting.

Finally, dispersion serves as a surrogate of shear wave viscosity and is estimated in a model-free approach as the slope of the shear wave speed as a function of shear wave frequency. It is worth noting that shear wave dispersion is a frequency-dependent measure. Herein, we considered dispersion in the frequency range of 100–200 Hz for liver shear wave elastography.<sup>22,23</sup>

Ultrasound images and spatially co-registered raw data were collected in three different acoustic settings and acoustic windows. HRI calculation was performed on raw RF data that form the final B-mode images as well as B-mode images captured in DICOM format. Typical images for HRI measurement contain the sagittal view of the liver and the right kidney (Figure 1). Attenuation coefficients and Nakagami coefficients were calculated from the same B-mode RF data acquired through an intercostal scan of the right liver lobe (Figures 2 and 3). Shear wave viscosity and dispersion were estimated from the raw IQ data, which produced an online elasticity measurement under shear wave elastography imaging-mode (ElastQ, Philips Healthcare, Andover, MA). Similar to attenuation imaging and Nakagami imaging, shear wave elastography measurements were also taken in the right lobe of the liver using an intercostal approach.

For each acoustic parameter, a region of interest (ROI) for final quantification was placed in a uniform area of liver parenchyma free of large vessels, masses, and acoustic artifacts. For each subject, all the parameters were calculated and averaged from at least three independent acquisitions.

A team of medical ultrasound scientists, blind to patient medical conditions and the results of MRI-PDFF, performed all offline ultrasound data processing and analysis.

### Magnetic Resonance Imaging

MRI was performed on a single 3 T MR scanner (Philips Ingenia 3 T, Philips Healthcare, Andover, MA). MRI-PDFF sequences were acquired according to a standard protocol using a three-dimensional volumetric sequence employed to derive T2\* and parametric maps of triglyceride fat fraction from a breath-hold acquisition. The parameters of the sequence for the single three-dimensional image with 22–28 axial images were as follows: TR, 5.6 msec; field of view, 35–40 cm; matrix, 160 × 140; bandwidth, 2367.4 Hz; flip angle, 3°; section thickness, 6 mm. We acquired data sets with six different echo times that ranged from 0.97 to 9.8 msec using a single breath-hold. The images were processed (Philips Intellispace, Philips Healthcare, Andover, MA) to create water, fat, R2\*, and fat fraction maps. Data analysis was performed by a fellowship-trained abdominal radiologist blinded to clinical history and ultrasound results. Circular regions ( $n = 9$ ) of interest (ROI) of approximately 1 cm in radius were placed in both right and left lobes of the liver, avoiding vascular structures; the mean fat fraction value over nine measurements was recorded for each subject (Figure 4). The median time interval between US and MRI was 43 days.

### Statistical Analyses

All statistical analyses were performed using statistical software SAS 9.4 (SAS Institute, Cary, NC). Demographic, biochemical, and imaging parameters (US and MRI) of patients were summarized as mean and standard deviation for continuous variables and numbers and percentages for categorical variables. Primary analysis included the correlation between quantitative US parameters detailed

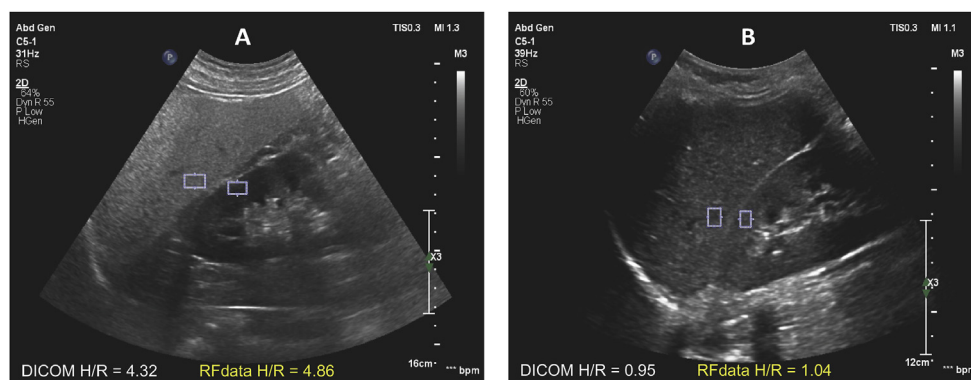


**Figure 1** Hepatorenal index DICOM and RF. A. Severe liver steatosis, HRI is 4.32 (PDFF = 25.4%). The difference in echogenicity between liver and renal cortical tissues is visibly significant. B. Healthy liver, HRI is 0.95 (PDFF = 1.3%). There is poor differentiation of echogenicity between liver and renal cortical tissues.

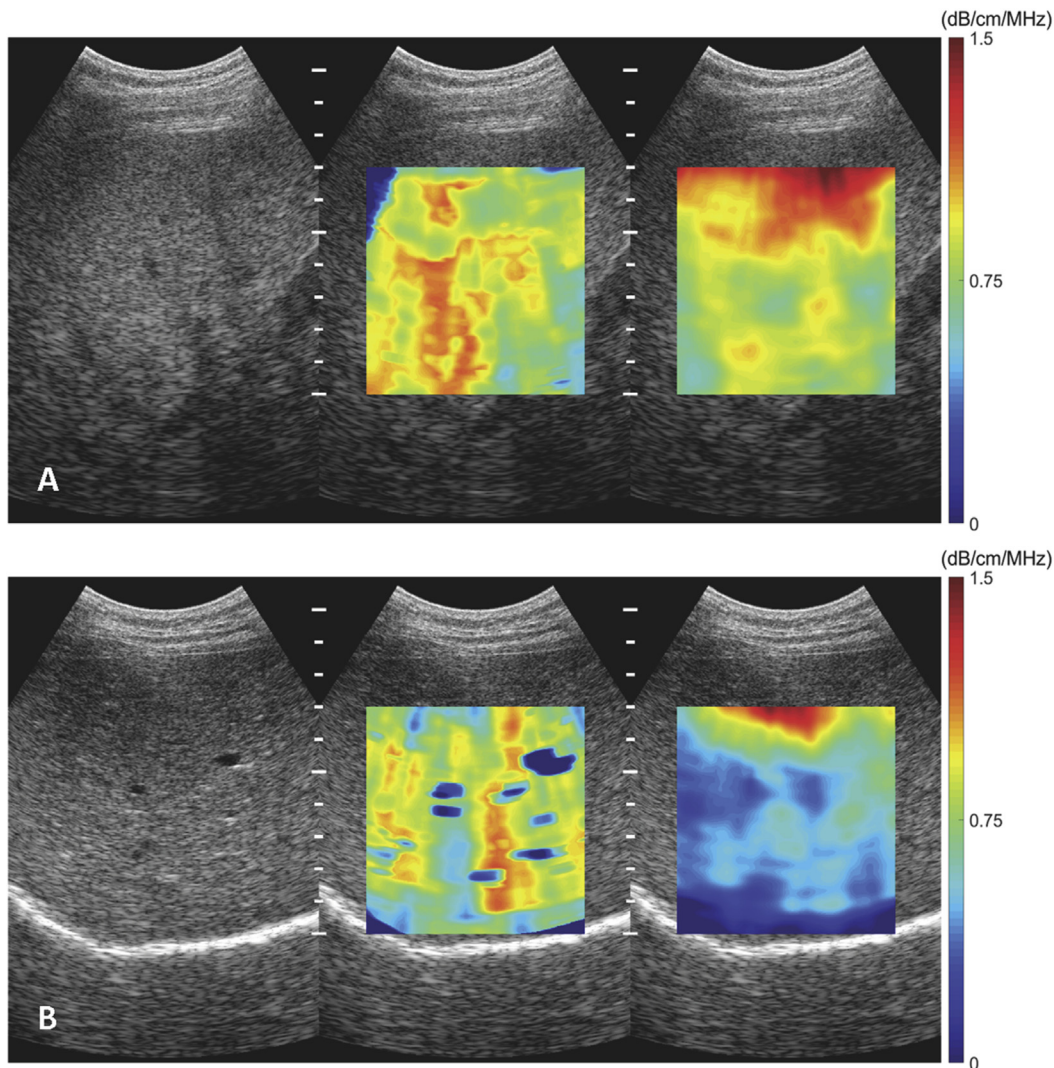


**Figure 2** Images of acoustic Attenuation coefficient. A. Severe liver steatosis, AttenQ = 0.80 dB/MHz/cm (PDFF = 25.4%). B. Healthy liver, AttenQ = 0.46 dB/MHz/cm (PDFF = 1.3%).

above with MRI-PDFF results. Furthermore, correlation analyses between BMI and laboratory results (ALT, AST, LDL, HbA1C) and imaging parameters were performed. Finally, we compared imaging parameters in patients with and without documented associated diseases and risk factors, namely, hypertension and diabetes, given association between these two pathologies and liver disease.<sup>24</sup>

A two-tailed  $P$ -value  $\leq 0.05$  was considered statistically significant.

## RESULTS

### Baseline Characteristics

Thirty-one patients undergoing quantitative liver US, followed by MRI, were consecutively enrolled in this prospective study. The mean ( $\pm$ SD) age and body mass index were 49.03 ( $\pm$  12.49) and 30.12 ( $\pm$  6.15), respectively. The baseline cohort characteristics are summarized in Tables 1 and 2.

### Comparing Imaging Measurements

Based on analyses of the data of 31 patients, the hepatorenal index (using raw RF data) showed a strong correlation with MRI-PDFF derivations of hepatic steatosis, with  $r = 0.828$  (Figure 5). However, the use of DICOM image-derived HRI showed a weaker correlation with MRI-PDFF,  $r = 0.626$  (95% CI). Additionally, a strong correlation between the attenuation coefficient and MRI-PDFF derivations of hepatic steatosis was identified,  $r = 0.743$  (Figure 6).

### Comparing Ultrasound and Metabolic Parameters

Hepatorenal index (DICOM) showed moderate correlation with ALT ( $r = 0.647$ ) and LDL ( $r = 0.537$ ). Attenuation coefficient showed moderate correlation with ALT ( $r = 0.518$ ) as well. Also, we found fair correlation between Nakagami/Nakagami harmonic parameters and BMI ( $r = 0.509$  and  $r = 0.476$ ). No additional correlations between imaging

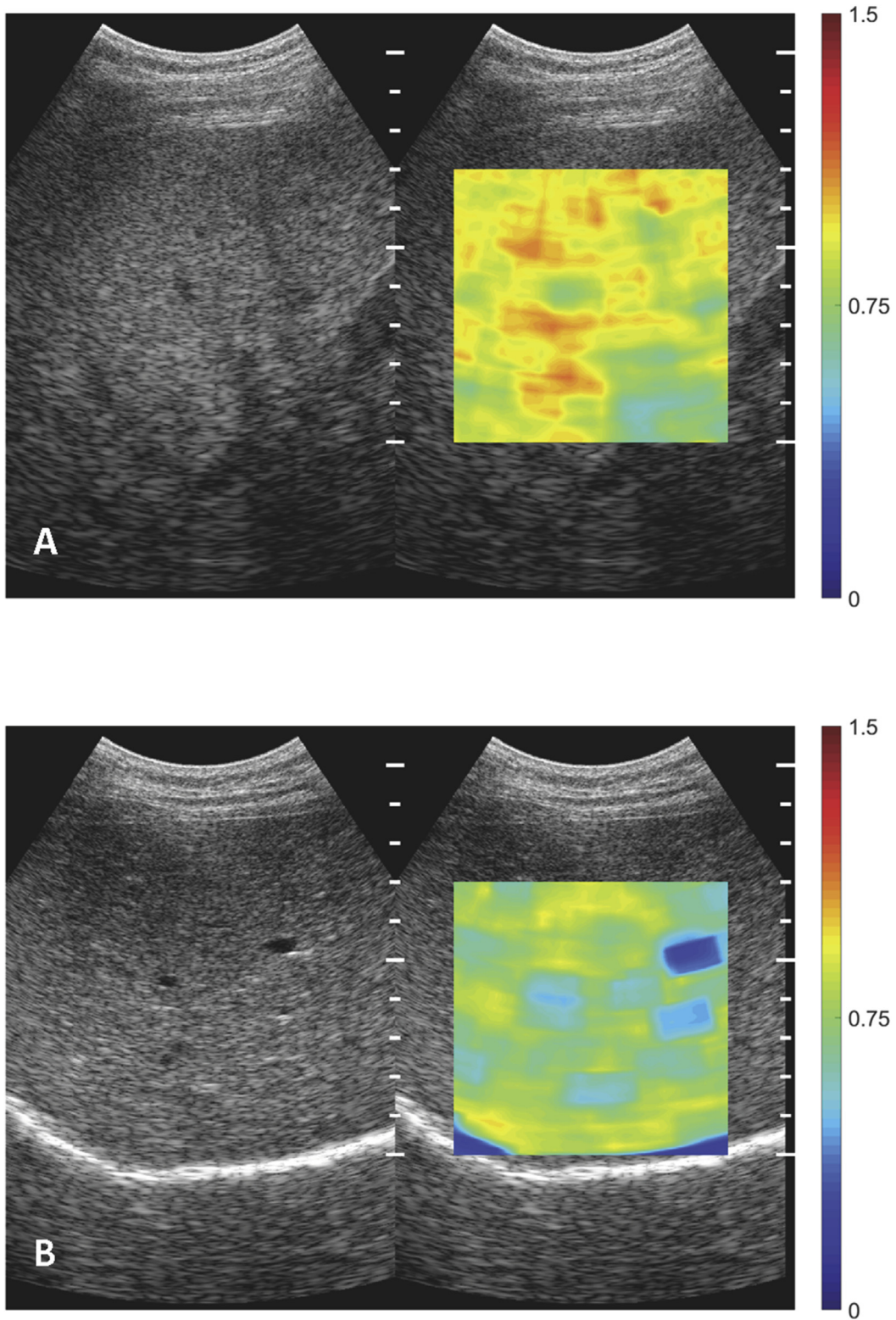


**Figure 3** Images of Nakagami parameters. A. Severe liver steatosis, Nakagami  $m = 0.95$  (PDFF = 25.4%). B. Healthy liver, Nakagami  $m = 0.78$  (PDFF = 1.3%).

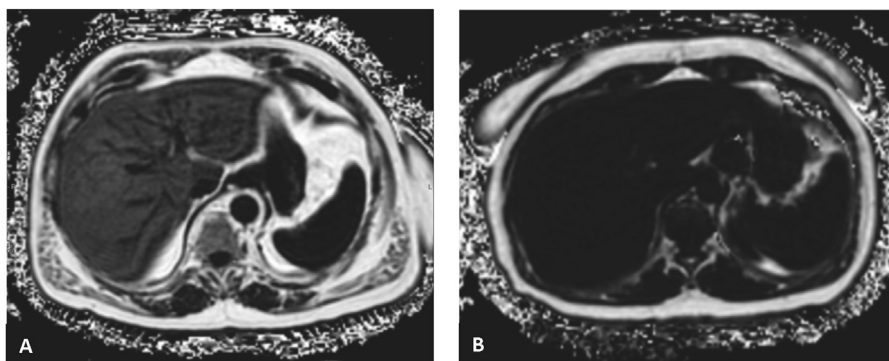


**Figure 4** MRI-PDFF images. **A.** Severe liver steatosis (PDFF = 25.4%), **B.** Normal liver (PDFF = 1.3%).

parameters and laboratory values of BMI were identified,  $r < 0.3$ . All data is summarized in Table 3.

### Comparing Ultrasound Parameters and Disease

In this study, we compared the quantitative imaging data of two groups of patients. The first was patients with and without diabetes mellitus (DM). T-test analysis showed no statistically significant difference between these groups and any quantitative US parameters (Table 4).

The second group compared patients with and without arterial hypertension. While no significant differences in hepatorenal indices (DICOM and RF) were found, there were significant differences between Nakagami, Nakagami harmonic parameter's, and acoustic attenuation coefficient of patients with and without hypertension ( $P$ -values = 0.004, 0.007, 0.020, respectively).

### DISCUSSION

In our study, the quantitative ultrasound parameters of hepatorenal index and acoustic attenuation coefficient show a strong correlation with MRI-PDFF-derived measures of hepatic steatosis. However, Nakagami and Nakagami harmonic parameters, shear wave elastography-derived viscosity, and dispersion were poorly correlated with MRI-PDFF-derived measures of hepatic steatosis. Interestingly, Nakagami, Nakagami harmonic parameters, and acoustic attenuation were found to be significantly different in patients with and without hypertension, while moderate correlations were identified between quantitative US parameters and several metabolic parameters.

Different correlations with MRI-PDFF were observed in HRI measurements calculated using the two different types of co-registered data. Compared to HRI-RF measurement, HRI-DICOM measurement had a weaker correlation with MRI-PDFF ( $r = 0.626$  vs.  $r = 0.828$ ). In this study, the operators were given the freedom to adjust system settings (gain, TGC, focus, depth, AutoScan, etc.) to optimize B-mode image quality for an individual subject and their preference during HRI data acquisition. The underperformance of the RF intensity signal before B-mode formation and sub-optimal user settings (e.g., over-gain or under-gain globally and locally). System processing and user settings can limit the data dynamic range, resulting in compromised HRI performance and potentially inaccurate diagnosis. In many early publications of diagnostic accuracy studies on HRI for liver steatosis assessment, authors only had access to final B-mode images for HRI calculation.<sup>25-28</sup> To

**Table 1** Demographical, Medical History, Imaging, and Biochemical Characteristics of Study Patients.

Characteristic*	Patients (n = 31)
<b>Demographic</b>	
Age at US/MRI exam, mean (SD)	49.03 (± 12.49)
Male, n (%)	10 (32.3)
Female, n (%)	21 (67.7)
<b>Medical history</b>	
Clinically expected NAFLD/NASH, n (%)	11 (35.4)
Diabetes	8 (25.8)
Hypertension	9 (29.0)
<b>Imaging</b>	
MRI-PDFF (%), median (IQR)	5.4222 (7.2944)
<b>Biochemical profile</b>	
AST (U/l), median (IQR)	26.5 (20.75)
ALT (U/l), median (IQR)	27.5 (36.0)
AST/ALT ratio, median (IQR)	1.095 (0.505)
Bilirubin (mg/dL), median (IQR)	0.45 (0.275)
Hgb A1C (%), median (IQR)	6.05 (2.075)
LDL (mg/dL), median (IQR)	82 (62.5)

Abbreviations employed in table: AST, Aspartate aminotransferase; ALT, Alanine aminotransferase; BMI, Body mass index; IQR, Interquartile range; HDL, High-density lipoprotein; Hgb A1C, Hemoglobin A1C (glycated hemoglobin); LDL, Low-density lipoprotein; NAFLD, Non-alcoholic fatty liver disease; NASH, Non-alcoholic steatohepatitis; SD, Standard deviation

**Table 2 Distribution of Correlation (r) of US and MRI-PDFF Imaging.**

	MRI-PDFF
Hepatorenal index (DICOM)	0.6269
Hepatorenal index (RF)	0.8289
Acoustic attenuation coefficient	0.7600
Nakagami coefficient	0.4778
Nakagami coefficient harmonic	0.4763
Shear wave dispersion (100–200 Hz)	0.3223
Viscosity	0.1837

minimize the user setting introduced measurement variability, operators were not allowed to change scanner settings throughout the study. The comparison results from this study suggest that RF-based HRI calculation rival

B-mode based calculation as the user will have more flexibility in optimizing image quality, while maintaining high fidelity in HRI measurement.

NAFLD has emerged as the leading cause of chronic liver disease in the United States.<sup>29</sup> It is defined as a spectrum of diseases, from hepatic steatosis that can progress to non-alcoholic steatohepatitis (NASH), fibrosis, cirrhosis, and even hepatocellular carcinoma.<sup>30</sup> NASH presents significant health, economic, and social problems to those affected, their families, and society.<sup>31</sup> While percutaneous liver biopsy is the gold standard in the detection and diagnosis of NAFLD, a biopsy is invasive with significant risks and several inherent limitations in accuracy.<sup>32</sup>

Therefore, other non-invasive imaging methods, such as ultrasound and MRI, are being investigated and developed for estimating liver fat content and diagnosing NAFLD and NASH.<sup>33</sup> MRI has been established as an accurate

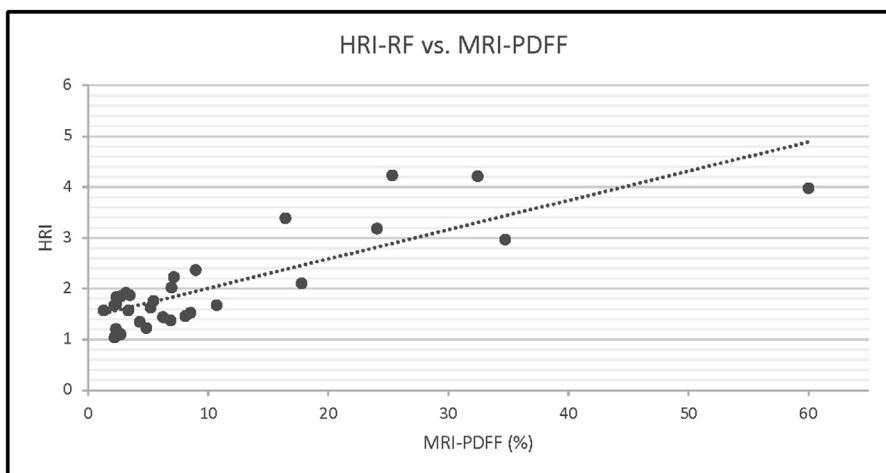


**Figure 5** There is a strong correlation between hepatorenal index (HRI) and MRI-PDFF ( $r > 0.7$ ).

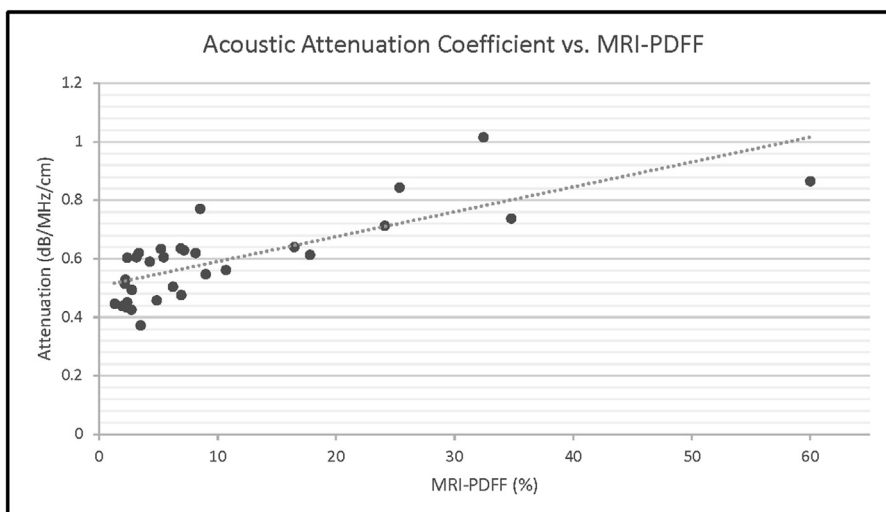


**Figure 6** There is a strong correlation between acoustic attenuation and MRI-PDFF ( $r > 0.7$ ).

**Table 3 Correlation (r) Between Imaging Parameters and BMI/laboratory Results.**

	BMI	LDL	ALT	AST	HbA1c
MRI-PDFF	-0.051	0.075	0.354	0.357	-0.025
HRI-RF	-0.065	-0.153	-0.163	-0.176	-0.295
HRI-D	-0.109	0.537	0.647	0.443	-0.216
Nakagami	0.509	0.128	0.365	0.150	0.325
Nakagami harmonic	0.476	0.080	0.316	0.096	0.267
Attenuation	0.047	0.022	0.518	0.438	0.237
Voigt viscosity 100 & 150 Hz	0.292	0.072	0.402	0.385	-0.063
Voigt viscosity 100 & 200 Hz	0.273	-0.026	0.492	0.300	-0.274
Voigt viscosity 100 to 200 Hz	0.295	0.028	0.452	0.313	-0.230
Dispersion-100-150 Hz	0.080	0.001	-0.101	-0.010	-0.300
Dispersion-150-200	-0.040	-0.068	0.159	-0.028	-0.383
Dispersion-100-200 Hz	0.051	0.032	0.021	-0.046	-0.295
Viscosity	0.377	0.532	0.191	0.086	0.194

**Table 4 Comparison of Quantitative US Imaging Parameters and Diabetes Mellitus and Hypertension.**

	Diabetes (mean and SD)	Non-diabetes (mean and SD)	P-value
MRI-PDFF	7.531 (5.518)	11.135 (14.082)	0.5472
HRI-RF	1.706 (0.301)	2.136 (0.985)	0.3056
HRI-DICOM	1.201 (0.141)	1.492 (0.534)	0.2017
Nakagami	0.909 (0.052)	0.872 (0.056)	0.1616
Nakagami harmonic	0.997 (0.032)	0.969 (0.048)	0.1824
Attenuation	0.596 (0.127)	0.594 (0.150)	0.9740
Voigt viscosity 100 & 150 Hz	2.169 (0.294)	2.160 (0.332)	0.954
Voigt viscosity 100 & 200 Hz	2.500 (0.295)	2.592 (0.358)	0.599
Voigt viscosity 100-200 Hz	2.454 (0.307)	2.509 (0.347)	0.744
Dispersion-100-150 Hz	13.221 (2.612)	12.746 (2.228)	0.676
Dispersion-150-200 Hz	14.280 (1.623)	14.977 (2.621)	0.575
Dispersion-100-200 Hz	11.699 (1.364)	11.923 (1.851)	0.800
Viscosity	1.7 (0.543)	2.033 (0.641)	0.289
	Hypertension (mean and SD)	Non-hypertension (mean and SD)	P-value
MRI-PDFF	16.737 (18.994)	8.246 (9.585)	0.1093
HRI-RF	2.245 (1.180)	1.979 (0.801)	0.4862
HRI-DICOM	1.428 (0.460)	1.436 (0.516)	0.9692
Nakagami	0.927 (0.043)	0.863 (0.052)	0.0046
Nakagami Harmonic	1.011 (0.029)	0.961 (0.045)	0.0074
Attenuation	0.694 (0.114)	0.560 (0.138)	0.0203
Voigt viscosity 100 & 150 Hz	2.131 (0.292)	2.169 (0.335)	0.7863
Voigt viscosity 100 & 200 Hz	2.473 (0.219)	2.586 (0.372)	0.4574
Voigt viscosity 100-200 Hz	2.421 (0.243)	2.508 (0.359)	0.5573
Dispersion-100-150 Hz	12.795 (2.783)	12.890 (2.167)	0.9253
Dispersion-150-200 Hz	14.082 (2.153)	14.874 (2.604)	0.4735
Dispersion-100-200 Hz	11.301 (1.740)	11.945 (1.760)	0.4056
Viscosity	1.9 (0.355)	1.977 (0.690)	0.7802

method for the evaluation of hepatic steatosis.<sup>34</sup> However, MRI is significantly more expensive than US, limited in its availability, and offers less flexibility in the physical locations where it may be applied, thereby limiting its role in routine NAFLD diagnosis. US has been widely used for initial screening of fatty liver and detecting NAFLD due to its availability, non-invasive nature, and low cost.<sup>35</sup> Previous studies on the use of conventional US for detecting fatty liver show sensitivities and specificities between 60%–94% and 66%–95%, respectively, demonstrating that its common application does not represent an adequate diagnostic tool for diagnosing, let alone quantifying, hepatic steatosis.<sup>36</sup> The development of quantitative ultrasound (QUS) aimed at improving diagnostic accuracy and the capacity to quantify liver fat is a promising, emerging application of this modality.<sup>37</sup>

Quantitative US techniques can be classified as image-based analysis and the raw-radiofrequency data acquisition from the scanner directly.<sup>38</sup> To date, similar to the results presented herein, attenuation coefficient has been reported to correlate with the degree of hepatic steatosis in preclinical models.<sup>39</sup> Furthermore, HRI has been reported to correlate with liver biopsy assessments of hepatic steatosis,<sup>40</sup> again echoing the results of this work. Once integrated into a commercial product, this technique may be performed by either ultrasound technologist or radiologist in order to deliver real-time fat quantification, relevant to the diagnosis and monitoring of chronic liver disease.

In the current study, the primary goal of which was to compare current QUS techniques with MRI-PDFF for the assessment of hepatic steatosis has some limitations. These include the fact that the cohort of participants was relatively small; however, this pilot-scale validation supports future inquiry utilizing larger datasets. Moreover, we did not compare QUS directly to liver biopsy (gold standard) for NAFLD detection; instead, we employed MRI-PDFF, a quantitative technique that has been demonstrated to be highly accurate in the diagnosis of liver steatosis.<sup>41</sup> Also, while this study was not designed to compare quantitative US parameters in patients with and without hypertension and diabetes, these early results are intriguing and warrant further investigation. Finally, the time interval between US and MRI (43 days on average) may have introduced a potentially confounding variable.

Hepatorenal index and acoustic attenuation coefficient correlate well with MRI-PDFF-derived measurements of hepatic steatosis. QUS represents a relatively inexpensive, highly flexible, portable modality that is well suited to evaluate the large populations affected by NAFLD. The results presented herein support the conclusion that quantitative ultrasound is a promising tool for the diagnosis and assessment of patients with NAFLD.

## CREDIT AUTHORSHIP CONTRIBUTION STATEMENT

Artem Kaliaev (Methodology, Validation, Formal analysis, Resources, Data Curation, Writing - Original Draft, Writing - Review & Editing, Visualization, Project administration). Wilson Chavez (Formal analysis, Resources, Writing - Review & Editing, Visualization, Project administration). Jorge Soto (Conceptualization, Writing - Review & Editing, Supervision). Fahimul Huda (Writing - Review & Editing, Visualization). Hua Xie (Software, Validation, Investigation, Data Curation, Writing - Review & Editing, Visualization). Man Nguyen (Software, Validation, Investigation, Data Curation, Writing - Review & Editing, Visualization). Vijay Shamdasani (Term, Investigation, Funding acquisition). Stephan Anderson (Term, Conceptualization, Methodology, Investigation, Writing - Review & Editing, Supervision, Funding acquisition).

## CONFLICTS OF INTEREST

The authors (Hua Xie, Man Nguyen, and Vijay Shamdasani) of this manuscript declare relationships with Philips Healthcare.

No conflicts of interest: Artem Kaliaev, Stephan Anderson, Wilson Chavez, Jorge Soto, Fahimul Huda.

## ACKNOWLEDGEMENTS

None.

## FUNDING

This study has received funding by Philips Healthcare, USA.

## GUARANTOR

The scientific guarantor of this publication is Stephan Anderson, MD ([Stephan.Anderson@bmc.org](mailto:Stephan.Anderson@bmc.org)).

## STATISTICS AND BIOMETRY

No complex statistical methods were necessary for this article.

## INFORMED CONSENT

Written informed consent was obtained from all patients in this study.

## ETHICAL APPROVAL

Institutional Review Board approval was obtained (IRB Protocol #H-37725 Approval date: 07/26/2018).

## METHODOLOGY

- Prospective
- Diagnostic study
- Performed at one institution

## REFERENCES

1. Wieckowska A, Feldstein AE. Diagnosis of nonalcoholic fatty liver disease: invasive versus noninvasive. *Semin Liver Dis.* 2008;28:386–395.
2. Mala D, Yamasandhi J. Nonalcoholic fatty liver disease and type 2 diabetes mellitus. *Indian J Endocrinol Metabol.* 2018;22:421–428.
3. Calzadilla Bertot L, Adams LA. The natural course of non-alcoholic fatty liver disease. *Int J Mol Sci.* 2016;17:774.
4. Younossi ZM, Blissett D, Blissett R, et al. The economic and clinical burden of nonalcoholic fatty liver disease in the United States and Europe. *Hepatology.* 2016;64:1577–1586.
5. Janiec DJ, Jacobson ER, Freeth A, Spaulding L, Blaszyk H. Histologic variation of grade and stage of non-alcoholic fatty liver disease in liver biopsies. *Obes Surg.* 2005;15:497–501.
6. Kleiner DE, Brunt EM, Van Natta M, et al. Nonalcoholic Steatohepatitis Clinical Research Network. Design and validation of a histological scoring system for nonalcoholic fatty liver disease. *Hepatology.* 2005;41:1313–1321.
7. Li Q. Current status of imaging in nonalcoholic fatty liver disease. *World J Hepatol.* 2018;10:530–542.
8. Sasso M, Miette V, Sandrin L, Beaugrand M. The controlled attenuation parameter (CAP): a novel tool for the non-invasive evaluation of steatosis using Fibroscan®. *Clin Res Hepatol Gastroenterol.* 2012;36:13–20.
9. Mehta SR, Thomas EL, Bell JD, Johnston DG, Taylor-Robinson SD. Non-invasive means of measuring hepatic fat content. *World J Gastroenterol.* 2008;14:3476–3483.
10. Kim M, Kang BK, Jun DW. Comparison of conventional sonographic signs and magnetic resonance imaging proton density fat fraction for assessment of hepatic steatosis. *Sci Rep.* 2018;8:7759.
11. Zelber-Sagi S, Webb M, Assy N, et al. Comparison of fatty liver index with noninvasive methods for steatosis detection and quantification. *World J Gastroenterol.* 2013;19:57–64.
12. Chauhan A, Sultan LR, Furth EE, Jones LP, Khungar V, Sehgal CM. Diagnostic accuracy of hepatorenal index in the detection and grading of hepatic steatosis. *J Clin Ultrasound.* 2016;44:580–586.
13. Kwon HJ, Kim KW, Jung JH, et al. Noninvasive quantitative estimation of hepatic steatosis by ultrasound: a comparison of the hepatorenal index and ultrasound attenuation index. *Med Ultrason.* 2016;18:431–437.
14. Kanayama Y, Kamiyama N, Maruyama K, Sumino Y. Real-time ultrasound attenuation imaging of diffuse fatty liver disease. *Ultrasound Med Biol.* 2016;39:692–705.
15. Hafez H, Anderson Z, Herd J, et al. Algorithm for estimating the attenuation slope from backscattered ultrasonic signals. In: *Proceedings - IEEE Ultrasonics Symposium.* 2009:1–4, 10.1109.
16. Tsui PH, Zhou Z, Lin YH, Hung CM, Chung SJ, Wan YL. Effect of ultrasound frequency on the Nakagami statistics of human liver tissues. *PLoS One.* 2017;12:e0181789.
17. Wan T, Liang Y. Application of ultrasound Nakagami imaging for the diagnosis of fatty liver. *J Med Ultrasound.* 2016;24:1016.
18. Tai Z, Wan D, Tseng Y, et al. Hepatic steatosis assessment with ultrasound small-window entropy imaging. *Ultrasound Med Biol.* 2018;44:1327–1340.
19. Shankar PM. A general statistical model for ultrasonic backscattering from tissues. *IEEE Trans. IEEE Transact Ultrasonics Ferroelectr Freq Control.* 2000;47:727–736.
20. Sugimoto K, Kobayashi Y, Itoi T. Assessment of liver elasticity and viscosity using shear waves induced by ultrasound radiation force: a study of hepatic fibrosis and inflammation in a rat model. *ECR, Scientific Exhibit.* 2017 [Poster presentation].
21. Yanrong G, Dong C, Lin H, et al. Evaluation of non-alcoholic fatty liver disease using acoustic radiation force impulse imaging elastography in rat models. *Ultrasound Med Biol.* 2017;43:2619–2628.
22. Barry CT, Hazard C, Hah Z, et al. Shear wave dispersion in lean versus steatotic rat livers. *J Ultrasound Med.* 2015;34:1123–1129.
23. Nightingale K, Rouze N, Rosenzweig S, Wang M, Abdelmalek M. Derivation and analysis of viscoelastic properties in human liver: impact of frequency on fibrosis and steatosis staging. *IEEE Trans Ultrason Ferroelectrics Freq Control.* 2015;62:165–175.
24. Wang Y, Zeng Y, Lin C, Chen Z. Hypertension and non-alcoholic fatty liver disease proven by transient elastography. *Hepatol Res.* 2016;46:1304–1310.
25. Shiralkar K, Johnson S, Bluth EI, Marshall RH, Domelles A, Gulotta MP. Improved method for calculating hepatic steatosis using the hepatorenal index. *J Ultrasound Med.* 2015;34:1051–1059.
26. Andre M, Han A, Heba E, et al. Accurate diagnosis of nonalcoholic fatty liver disease in human participants via quantitative ultrasound. In: *IEEE International Ultrasonics Symposium, Chicago, IL, 2014.* 2014:2375–2377.
27. Festi D, Schiumerini R, Marzi L, et al. Review article: the diagnosis of non-alcoholic fatty liver disease – availability and accuracy of non-invasive methods. *Aliment Pharmacol Ther.* 2013;37:392–400.
28. Marshall R, Eissa M, Bluth E, Gulotta P, Davis N. Hepatorenal index as an accurate, simple, and effective tool in screening for steatosis. *Am J Roentgenol.* 2021;199:997–1002.
29. Chalasani N, Younossi Z, Lavine JE. The diagnosis and management of non-alcoholic fatty liver disease: practice guideline by the American Association for the study of liver diseases, American college of gastroenterology, and the American gastroenterological association. *Hepatology.* 2012;55:5–23.
30. Adams LA, Lymp JF, Sauger JSt. The natural history of nonalcoholic fatty liver disease: a population-based cohort study. *Gastroenterology.* 2005;129:113–121.
31. Younossi Z, Tacke F, Arrese M, et al. Global perspectives on nonalcoholic fatty liver disease and nonalcoholic steatohepatitis. *Hepatology.* 2018;69:2672–2682.
32. Martinez SM, Crespo G, Navasa M, Forns X. Noninvasive assessment of liver fibrosis. *Hepatology.* 2011;53:325–335.
33. Nguyen D, Talwalkar JA. Noninvasive assessment of liver fibrosis. *Hepatology.* 2011;53:2107–2110.
34. Idilman IS, Keskin O, Celik A, Savas B, Elhan AH, Idilman R. A comparison of liver fat content as determined by magnetic resonance imaging-proton density fat fraction and MRS versus liver histology in non-alcoholic fatty liver disease. *Acta Radiol.* 2016;57:271–278.
35. Schwenzer NF, Springer F, Schraml C. Non-invasive assessment and quantification of liver steatosis by ultrasound, computed tomography and magnetic resonance. *J Hepatol.* 2009;51:433–445.
36. Lin S, Heba E, Wolfson T, et al. Noninvasive diagnosis of nonalcoholic fatty liver disease and quantification of liver fat using a new quantitative ultrasound technique. *Clin Gastroenterol Hepatol.* 2015;13:1337–1345.
37. Ozturk A, Grajo JR, Gee MS, et al. Quantitative hepatic fat quantification in non-alcoholic fatty liver disease using ultrasound-based

- techniques: a Review of literature and their diagnostic performance. *Ultrasound Med Biol*. 2018;44:2461–2475.
38. Yang KC, Liao YY, Tsui PH, Yeh CK. Ultrasound imaging in nonalcoholic liver disease: current applications and future developments. *Quant Imag Med Surg*. 2019;9:546–551.
39. Kwon HJ, Kim KW, Lee SL, et al. Value of the ultrasound attenuation index for noninvasive quantitative estimation of hepatic steatosis. *J Ultrasound Med*. 2013;32:229–235.
40. Xia MF, Yan HM, He WY, et al. Standardized ultrasound hepatic/renal ratio and hepatic attenuation rate to quantify liver fat content: an improvement method. *Obesity*. 2012;20:444–445.
41. Qu Y, Li M, Hamilton G, Zhang Y, Song B. Diagnostic accuracy of hepatic proton density fat fraction measured by magnetic resonance imaging for the evaluation of liver steatosis with histology as reference standard: a meta-analysis. *Eur Radiol*. 2020;29:5180–5189.